Supporting information with "Insights in the recalcitrance of theasinensin A to human gut microbial degradation" by Liu, de Bruijn, Sanders, Wang, Bruins, and Vincken.

Table S1. Theasinensin A (TSA) and Theaflavin-3,3′-digallate (TFDG) Contents in 15 Black Tea Samples and 6 Oolong Tea Samples.

Black tea				Oolong tea			
NO.	**Name & source**	**TSA (mg/g) [a]**	**TFDG (mg/g) [b]**	**NO.**	**Name & source**	**TSA (mg/g) [a]**	**TFDG (mg/g) [b]**
1	Jinjunmei, Fujian, China	6.30	2.56	1	Tieguanyin, Fujian, China	0.71	0.27
2	Lapsang souchong, Fujian, China	7.07	3.08	2	Baijiguan, Fujian, China	2.20	0.90
3	Dianhong, Yunnan, China	6.49	1.53	3	Bantianyao, Fujian, China	1.91	0.44
4	Qimen, Anhui, China	2.20	0.52	4	Shuijinggui, Fujian, China	2.24	0.79
5	Black tea, Guangxi, China [c]	2.38	0.68	5	Rougui, Fujian, China	3.41	0.65
6	Black tea, Fujian, China [c]	6.78	3.03	6	Tieluohan, Fujian, China	3.03	1.17
7	Zhenda, Fujian, China	1.05	0.95		**Average**	**2.25**	**0.70**
8	Fuyun, Fujian, China	2.79	0.97				
9	Wuyi, Fujian, China	1.30	2.20				
10	Minbei, Fujian, China	1.21	1.17				
11	Black tea, Kenya [c]	1.66	1.84				
12	Black tea, Indonesia [c]	1.59	1.98				
13	Black tea, Sri Lanka [c]	6.64	3.03				
14	Black tea, India [c]	5.44	3.55				
15	Lipton black tea, Wageningen, The Netherlands	2.72	1.54				
	Average	**3.71**	**1.91**				

[a] TSA content was expressed as mg per g dry weight of tea leaves, quantified using an external calibration curve of the purified TSA.
[b] TFDG content was expressed as mg per g dry weight of tea leaves, quantified using an external calibration curve of the TFDG standard.
[c] Brand names are unkown.

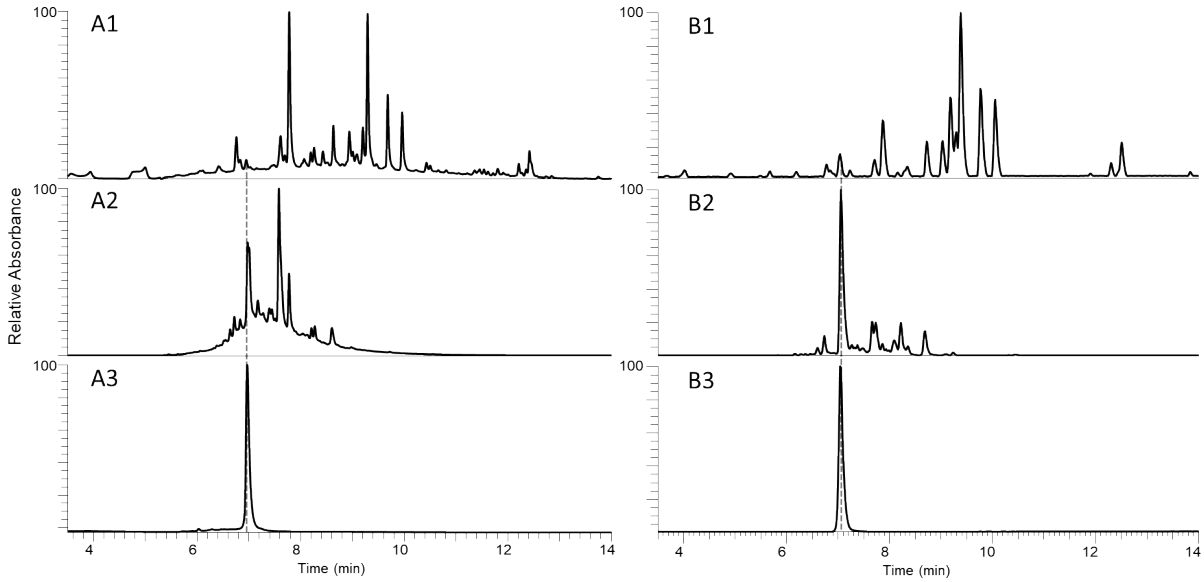

Figure S1. UHPLC-$UV_{280\,nm}$ (A1−A3) and UHPLC-MS base peak (B1−B3, negative ionization mode) chromatograms of decaffeinated black tea extract NO. 2 (A1, B1), pre-purified TSA after Flash chromatography (A2, B2), and TSA purified by preparative RP-HPLC (A3, B3).

The methods used for flash chromatography and preparative RP-HPLC are as follows:
The decaffeinated black tea extract was pre-purified using a Reveleris flash chromatography system (Grace, Columbia, USA). The sample was separated on a C18 column (40 μm, 40 g; Reveleris; Grace, Columbia, USA). Mobile phases consisting of 0.1% (*v/v*) formic acid in water (A) and 0.1% (*v/v*) formic acid in methanol (B) were used to elute the column at a flow rate of 40 mL/min. The elution program was set as follows: 0–4.5 min, isocratic on 10% (*v/v*) B; 4.5–14.5 min, linear gradient from 10% to 20% (*v/v*) B; 14.5–16 min, linear gradient from 20% to 50% v/v B; 16–21 min, linear gradient from 50% to 95% (*v/v*) B; 21-22.5 min, isocratic on 95% (*v/v*) B; 22.5–25.5 linear gradient from 95% to 10% (*v/v*) B; 25.5-28 min isocratic on 10% (*v/v*) B. The collected fractions were analysed by UHPLC-ESI-IT-MS (Thermo Fischer Scientific, San Jose, CA, USA) and those containing TSA were pooled. The organic solvent was evaporated under reduced pressure at 45 °C, and water was then removed by lyophilisation. Next, a Waters preparative RP-HPLC system (Waters, Milford, MA, USA) was used for the further purification of the pools obtained from Flash chromatography. The pools were solubilised at 50 mg/mL in a methanol/water (17:83, *v/v*) solution and injected (2.0–2.5 mL) on a Waters XBridge Prep C18 OBD column (19×250 mm, 5 μm). Mobile phase A was 0.1% (*v/v*)

formic acid in water and mobile phase B was 0.1% (*v/v*) formic acid in methanol were used to elute the column at a flow rate of 17 mL/min at room temperature. The elution program was as follows: 0–2.17 min, isocratic on 5% (*v/v*) B; 2.17–72.17 min, linear gradient from 5% to 15% (*v/v*) B; 72.17–75.67 min, linear gradient from 15% to 99 % (*v/v*) B; 75.67–93.17 min, isocratic on 99% (*v/v*) B; 93.17-96.67 min, linear gradient from 99% to 5% (*v/v*) B; 96.67-114.17 min isocratic on 5% (*v/v*) B. Data was acquired and analysed with MassLynx (version 4.1, Waters). The collected fractions were analysed by UHPLC-ESI-IT-MS and those containing TSA were pooled. The organic solvent was evaporated under reduced pressure at 45 °C, and water was removed by lyophilisation.

Supporting information with "Insights in the recalcitrance of theasinensin A to human gut microbial degradation" by Liu, de Bruijn, Sanders, Wang, Bruins, and Vincken.

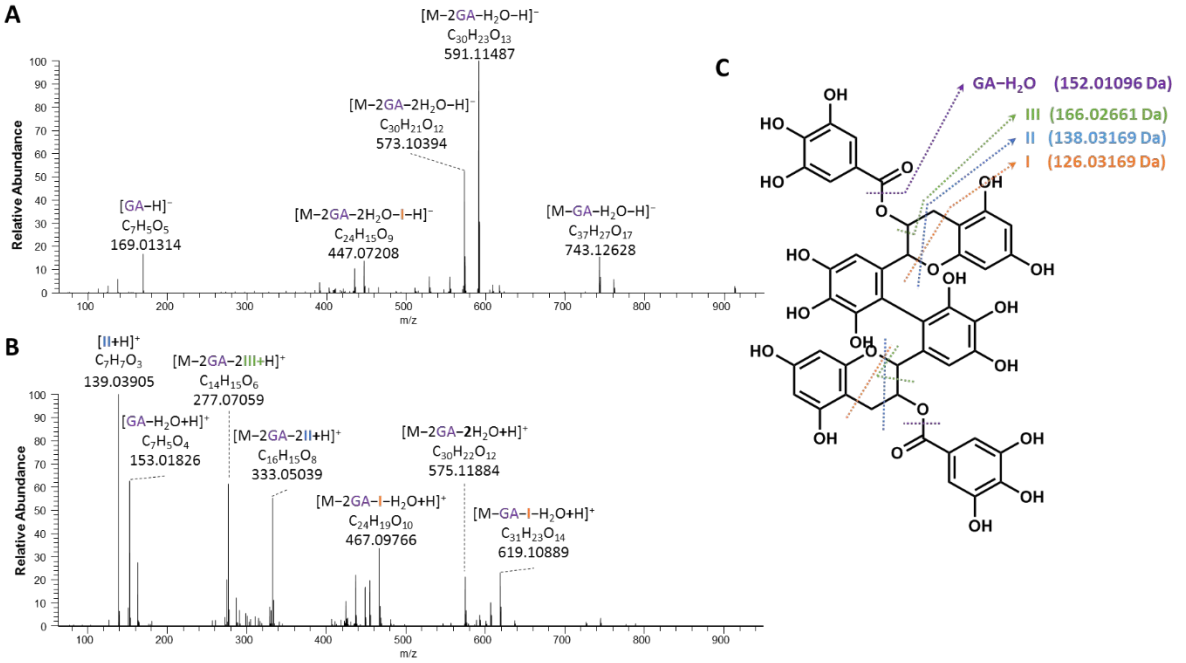

Figure S2. High resolution HCD fragmentation spectrum (NCE=35) of purified TSA in negative (A) and positive (B) ionization mode obtained from UHPLC-Q-Orbitrap-MS. The characteristic peaks are labelled with their corresponding fragmentation pathways (C).

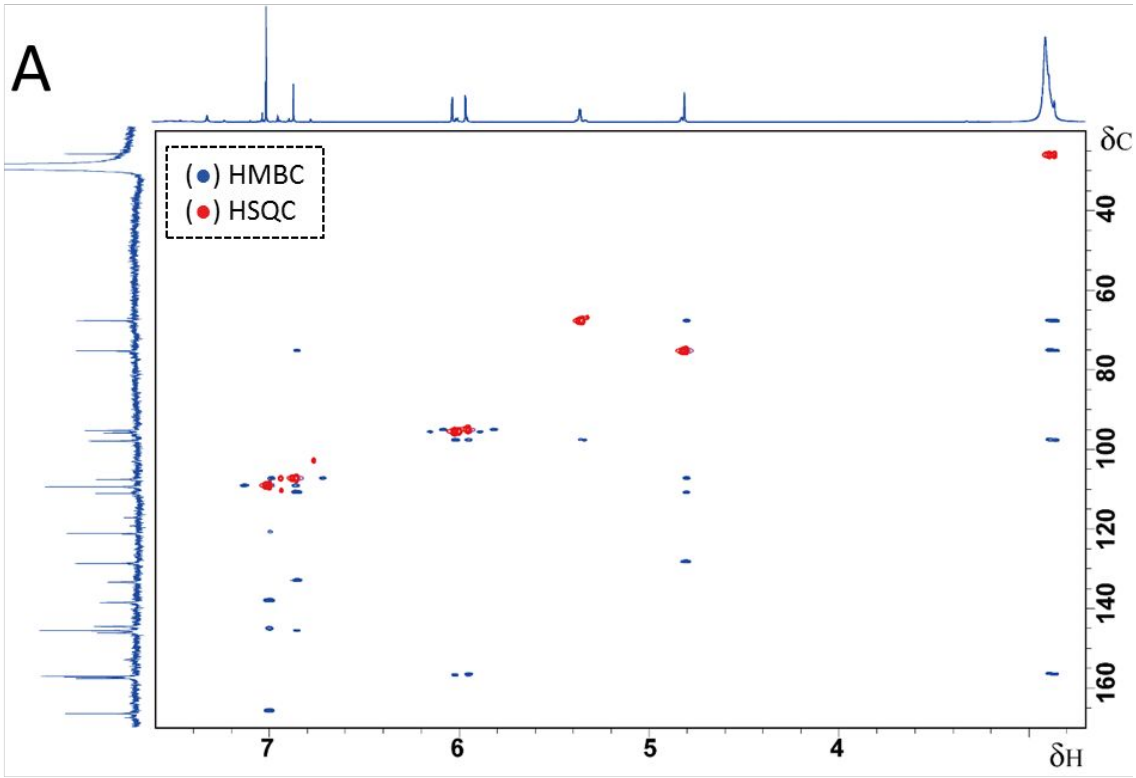

B

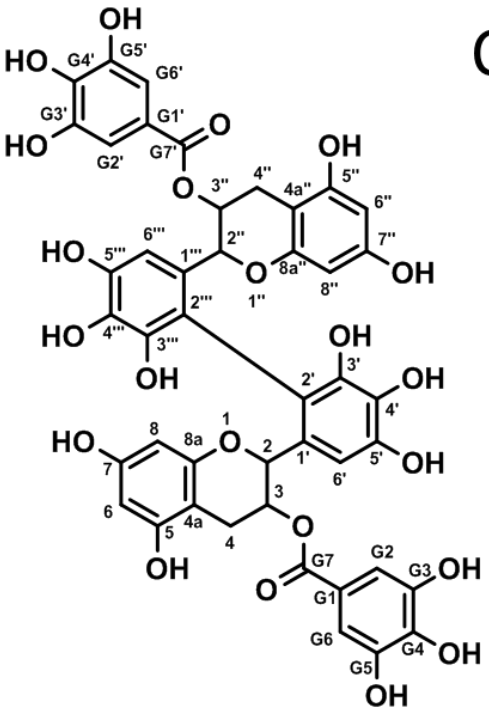

C

Position	δ_C	δ_H
A- and C-rings		
2 & 2''	75.2	4.80
3 & 3''	68.0	5.36
4 & 4''	26.3	2.91
4a & 4a''	97.5	
5 & 5''	156.5	
6 & 6''	95.1	5.96
7 & 7''	156.5	
8 & 8''	95.8	6.03
8a & 8a''	156.5	
B-ring		
1' & 1'''	128.3	
2' & 2'''	110.8	
3' & 3'''	144.6	
4' & 4'''	132.8	
5' & 5'''	146.2	
6' & 6'''	107.5	6.86
Galloyl group		
G1 & G1'	137.9	
G2 & G2'	109.1	7.00
G3 & G3'	145.6	
G4 & G4'	145.6	
G5 & G5'	145.6	
G6 & G6'	109.1	7.00
G7 & G7'	165.6	

Figure S3. NMR analysis of TSA in acetone-d_6 was performed on a Bruker Avance III 600 MHz spectrometer equipped with a cryogenic probe (Bruker BioSpin, Rheinstetten, Germany). Recorded 1D ^{1}H and ^{13}C, and 2D HSQC (red) and HMBC (blue) spectra (A), chemical structure of TSA (B), and NMR spectroscopic data for TSA (δ in ppm) (C).

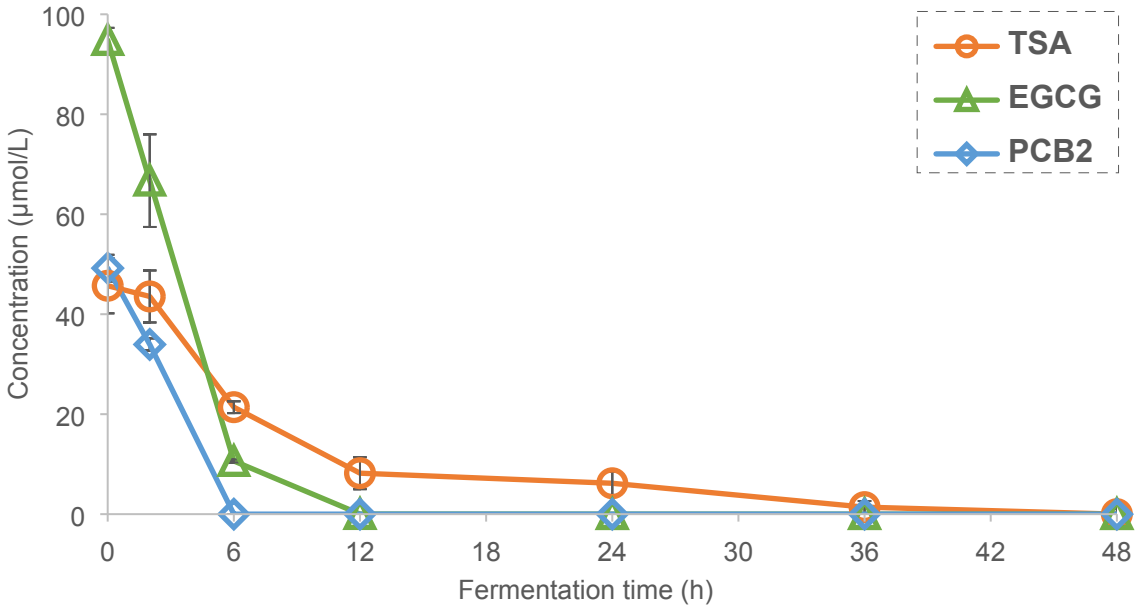

Figure S4. Changes in the concentrations of TSA, EGCG, and PCB2 during the fermentation. Error bars show standard deviation of three biological replicates.

Supporting information with "Insights in the recalcitrance of theasinensin A to human gut microbial degradation" by Liu, de Bruijn, Sanders, Wang, Bruins, and Vincken.

Table S2. Mass Spectrometric Data of Metabolites of TSA, EGCG, and PCB2 Tentatively Identified by UHPLC-Q-Orbitrap-MS.

id	Tentative identification	$[M-H]^-$ (*m/z*)	MS^2 [a]
M01	Theasinensin B	761.13617	591.11475; 609.12634; 453.08325; 169.01302; 327.05096; 339.05133
M02	Theasinensin C	609.12500	471.09274; 167.03378; 303.05090; 453.08359; 333.06113
M03	Theasinensin E	609.12506	471.09274; 167.03378; 303.05090; 453.08359; 333.06113
M04	Epigallocatechin	305.06680	125.02302; 137.02312; 146.95995; 167.03407; 219.06551
M05	Epicatechin	289.07181	109.02795; 123.04369; 125.02293; 151.03882; 97.02792
M06	1-(3′,4′,5′-Trihydroxyphenyl)-3-(2′′,4′′,6′′-trihydroxyphenyl)-propan-2-yl gallate	459.09369	267.09863; 129.10191; 169.01317; 223.10832; 307.08218
M07	1-(3′,4′,5′-Trihydroxyphenyl)-3-(2′′,4′′,6′′-trihydroxyphenyl)-propan-2-ol	307.08252	139.03874; 214.92589; 151.03882; 167.03387; 125.02300
M08	1-(3′,4′-Dihydroxyphenyl)-3-(2′′,4′′,6′′-trihydroxyphenyl)-propan-2-ol	291.08762	123.04369; 135.04385; 167.03362
M09	2-(3-(3,4-Dihydroxyphenyl)-2-hydroxy-1-(2,4,6-trihydroxyphenyl)propyl)-4-(3-(3,4-dihydroxyphenyl)-2-hydroxypropyl)benzene-1,3,5-triol	581.16687	291.08759; 125.02300; 167.03386; 333.09814; 455.13519
M10	2-(3,4-Dihydroxyphenyl)-8-(3-(3,4-dihydroxyphenyl)-2-hydroxy-1-(2,4,6-trihydroxyphenyl)propyl)chromane-3,5,7-triol	579.15143	291.08759; 409.09299; 125.02302
M11	2-(3-(3,4-dihydroxyphenyl)-2-hydroxy-1-(2,4,6-trihydroxyphenyl)propyl)-4-(2-hydroxy-3-(3-hydroxyphenyl)propyl)benzene-1,3,5-triol	563.15564	n.d.
M12	5-(3′,4′,5′-Trihydroxyphenyl)-γ-valerolactone	223.06055	91.05374; 171.78961;133.06442;122.70895
M13	5-(3′,4′-Dihydroxyphenyl)-γ-valerolactone	207.06607	75.00163; 87.92365; 103.91849; 118.99162; 147.04387
M14	5-(4′-Hydroxyphenyl)-γ-valerolactone	191.07103	n.d.
M15	4-Hydroxy-5-(3′,4′,5′-trihydroxyphenyl)-valeric acid	241.07146	124.02633; 111.01853; 169.09735; 129.10194; 153.10263
M16	4-Hydroxy-5-(3′,4′-dihydroxyphenyl)-valeric acid	225.07631	123.04369; 163.07510; 135.04396
M17	5-(3′,4′,5′-Trihydroxyphenyl)-valeric acid	225.07632	81.03294; 123.04369; 101.02281
M18	5-(3′,5′-Dihydroxyphenyl)-valeric acid	209.08165	n.d.
M19	5-(3′,4′-Dihydroxyphenyl)-valeric acid	209.08164	123.08006; 81.03296; 107.04872; 91.05378; 149.05963
M20	5-(4′-Hydroxyphenyl)-valeric acid	193.08691	121.02799; 90.92209; 175.07524; 147.08031; 106.04085

M21	3-(3′,5′-Dihydroxyphenyl)-propionic acid	181.05032	92.99213; 136.98221; 123.03127
M22	3-(3′,4′-Dihydroxyphenyl)-propionic acid	181.05040	92.99213; 136.98221; 123.03127
M23	3-(3′-Hydroxyphenyl)-propionic acid	165.05543	119.04870; 121.02797; 106.04082; 92.02517
M24	Gallic acid	169.01403	69.03293; 125.02317; 97.02796; 79.01718
M25	4-Hydroxybenzoic acid	137.02398	93.03298; 65.03806; 125.88489
M26	Pyrogallol	125.02412	69.03297; 67.01733; 124.01511; 97.02785; 79.01739

[a] MS^2 data are sorted in order of relative intensity; n.d., not detected.

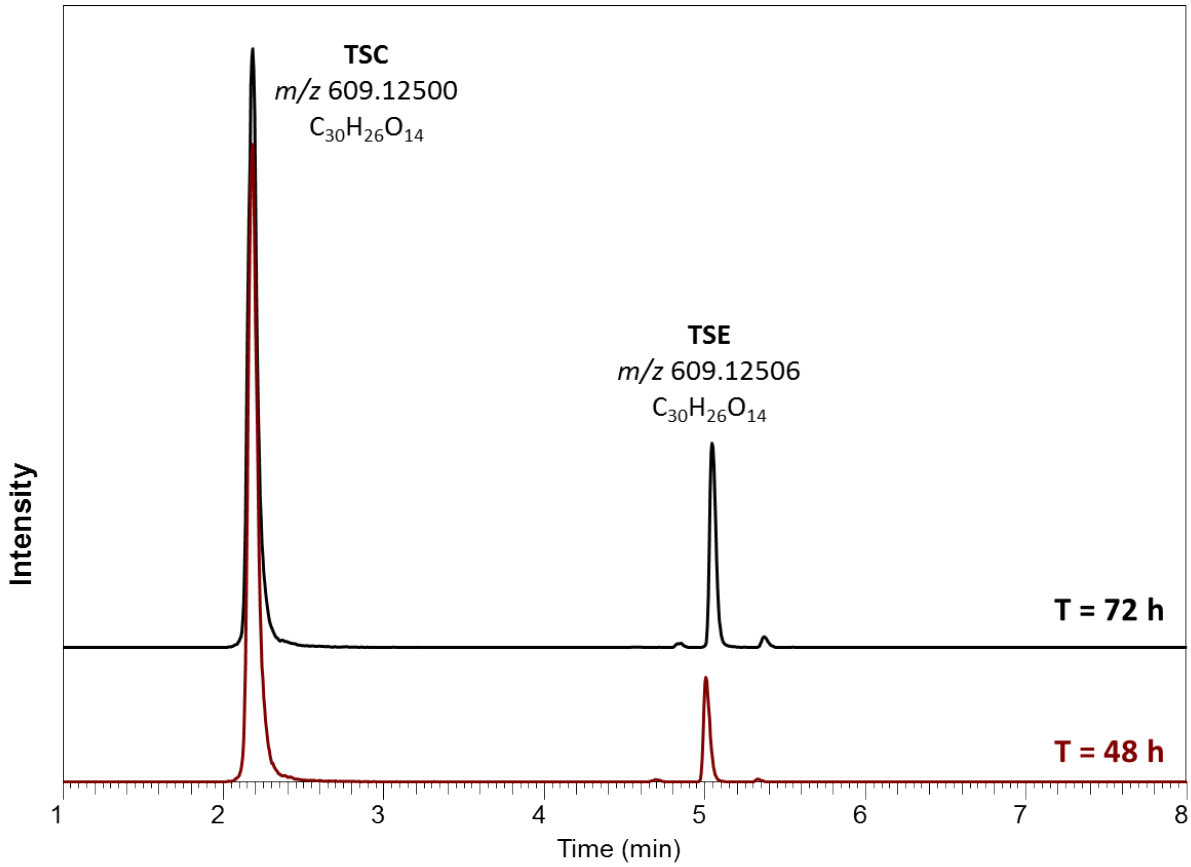

Figure S5. Extracted ion chromatograms of TSC (*m/z* 609.12500) and TSE (*m/z* 609.12506) in negative ion mode UHPLC-Q-Orbitrap-MS of TSA fermentation samples at fermentation times of 48 and 72 h.

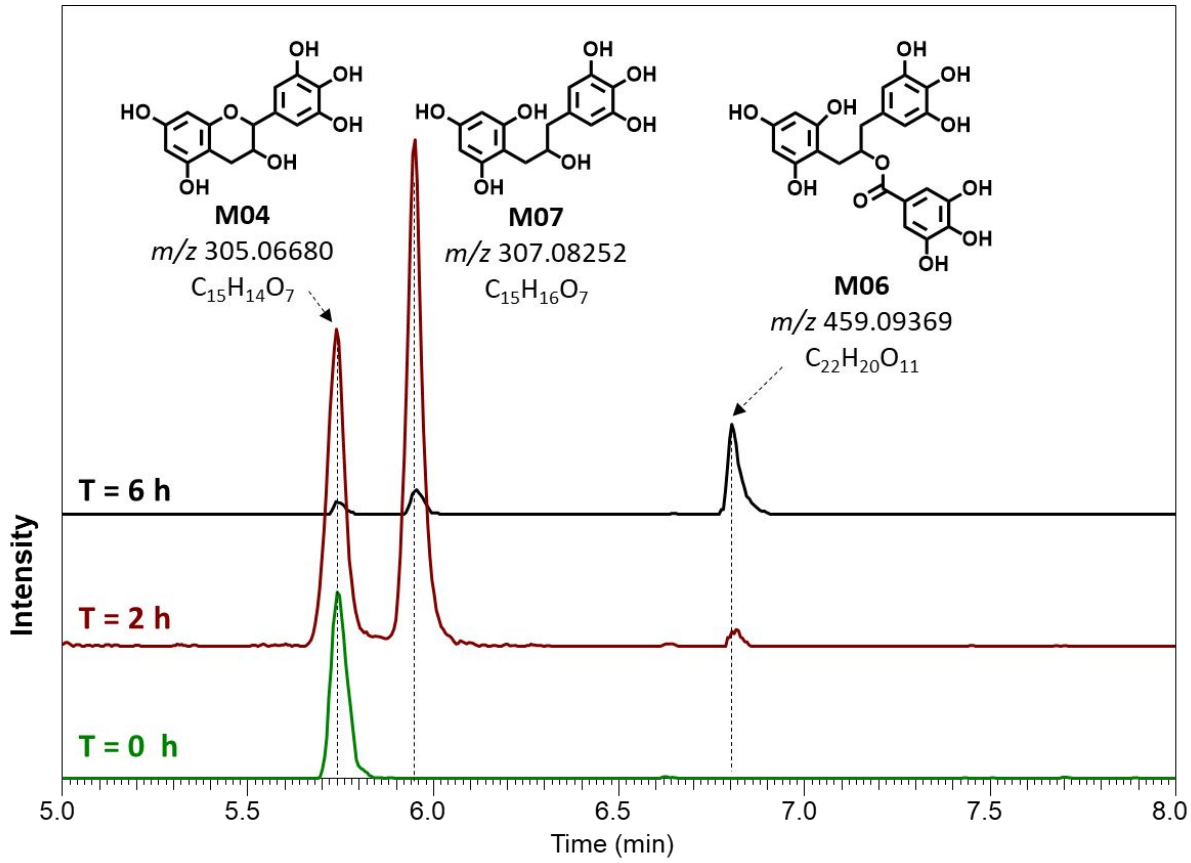

Figure S6. Extracted ion chromatograms of M04 (*m/z* 305.06680), M06 (*m/z* 459.09369), and M07 (*m/z* 307.08252) in negative ion mode UHPLC-Q-Orbitrap-MS of EGCG fermentation samples at fermentation times 0, 2, and 6 h.

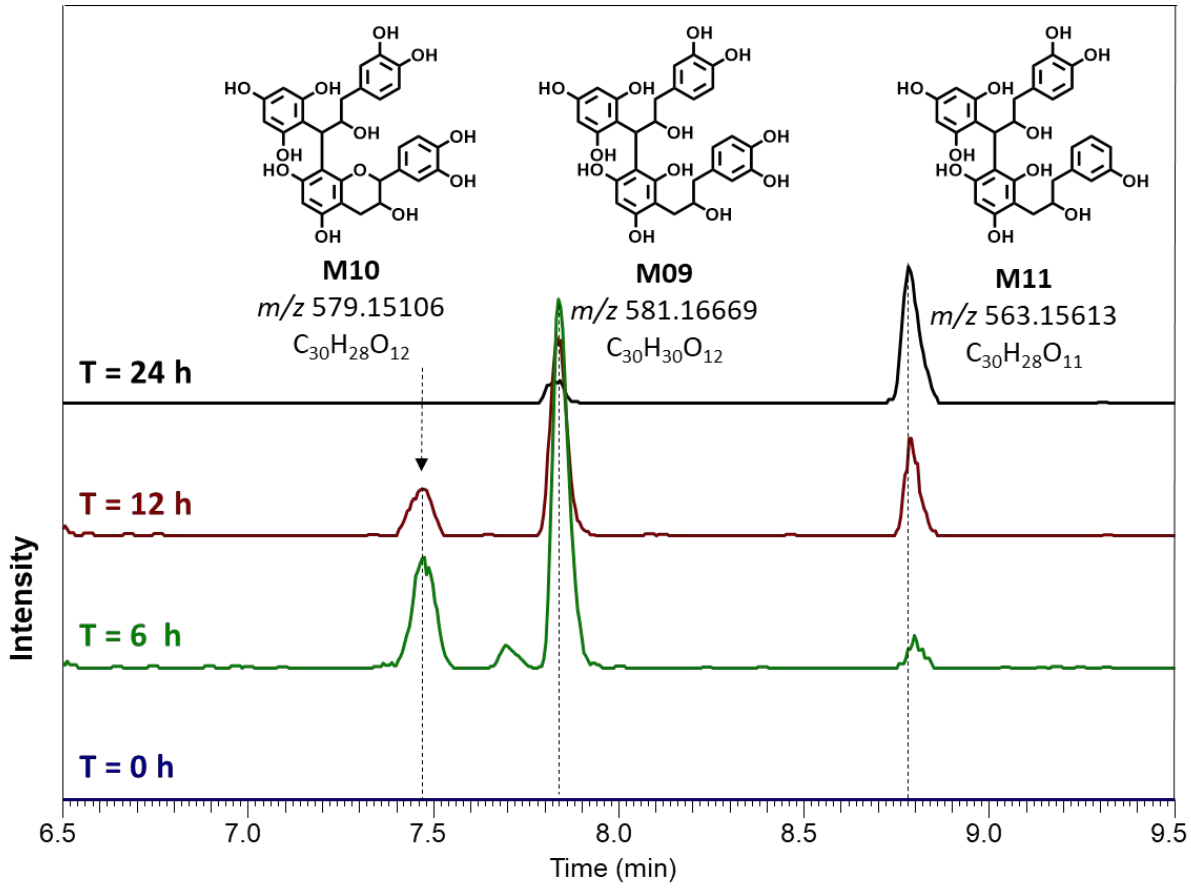

Figure S7. Extracted ion chromatograms of M09 (*m/z* 581.16669), M10 (*m/z* 579.15106), and M11 (*m/z* 563.15613) in negative ion mode UHPLC-Q-Orbitrap-MS of PCB2 fermentation samples at fermentation times 0, 6, 12, and 24 h. Note that for M10 and M11 just one possible positional isomer, with regards to C-ring opening and dehydroxylation, respectively, is shown.

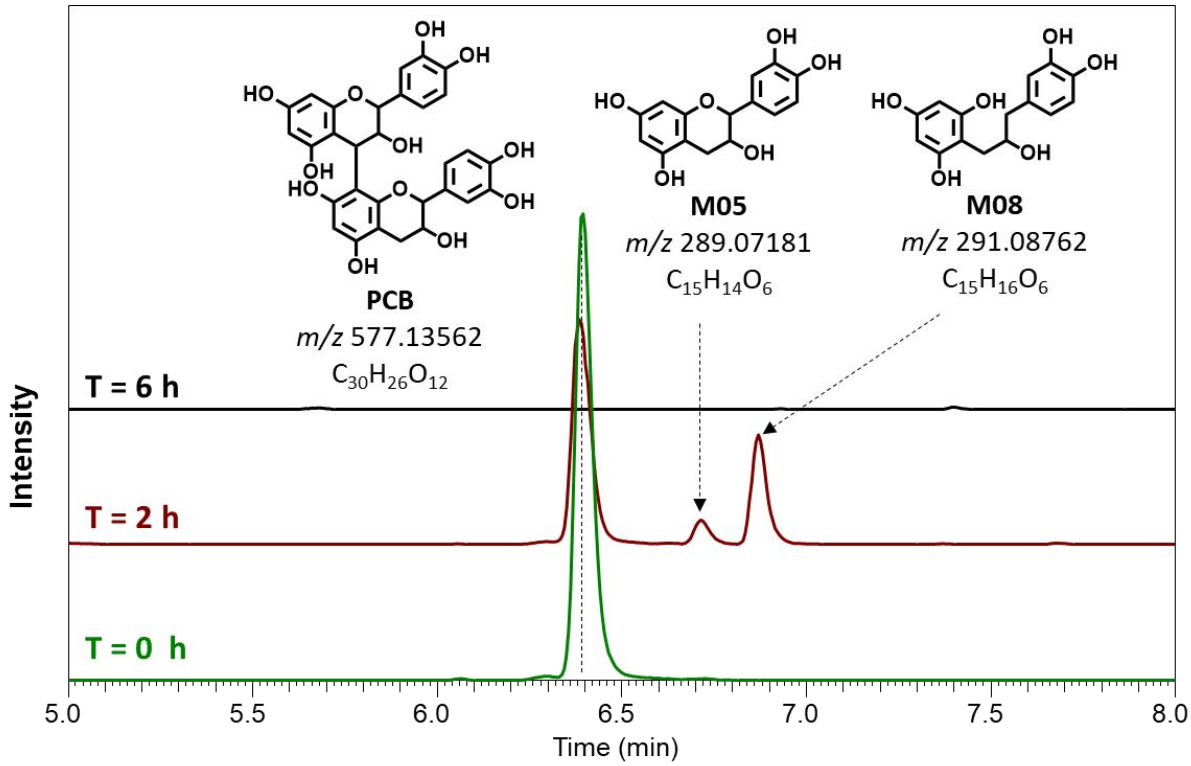

Figure S8. Extracted ion chromatograms of PCB2 (*m/z* 577.13562), M05 (*m/z* 289.07181), and M08 (*m/z* 291.08762) in negative ion mode UHPLC-Q-Orbitrap-MS of PCB2 fermentation samples at fermentation times 0, 2, and 6 h.

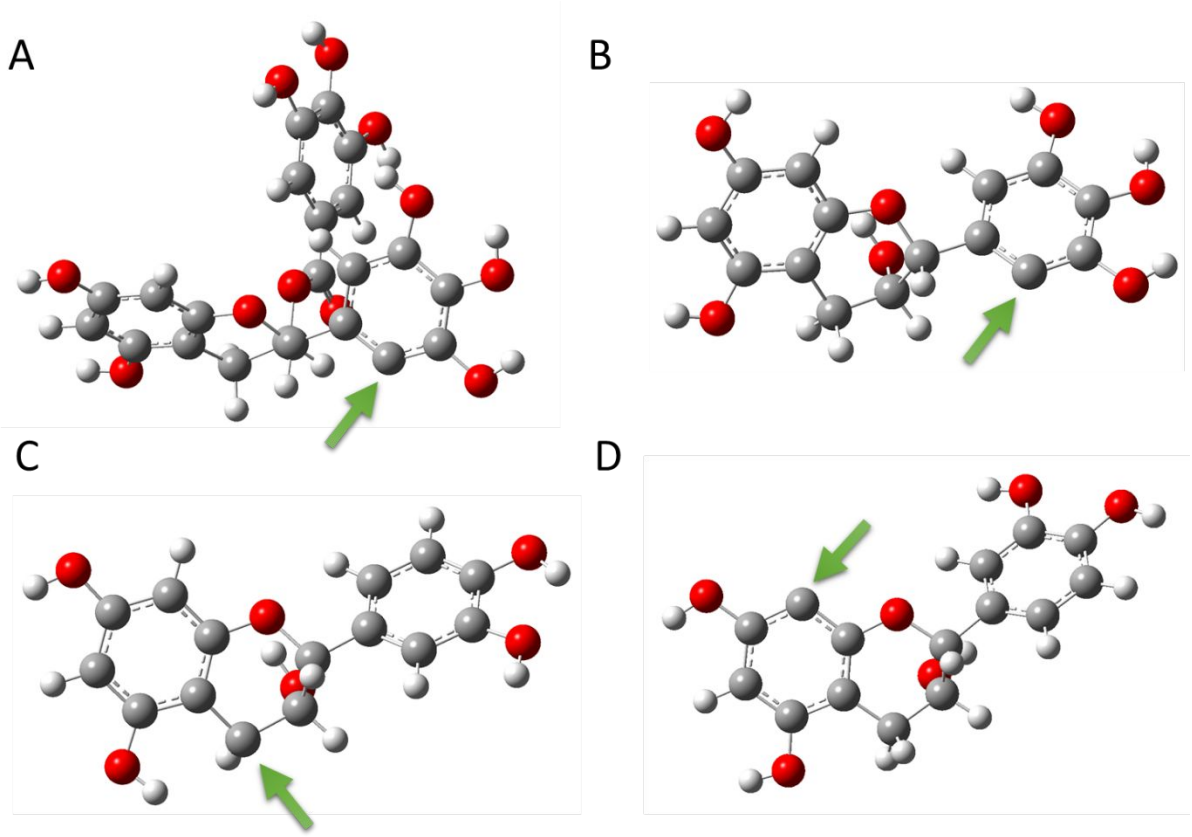

Figure S9. Optimized geometries of the interflavanic bond homolytically fissioned radicals of TSA (A), TSC (B), and PCB2 (C, upper unit; D, lower unit). The radical atoms are indicated with arrows.